Solving the mystery of the walk-off soliton

Mario Zitelli,[1,*] Fabio Mangini,[2] Mario Ferraro,[1] Oleg Sidelnikov[3], and Stefan Wabnitz[1,3]

[1] Department of Information Engineering, Electronics and Telecommunications (DIET), Sapienza University of Rome, Via Eudossiana 18, 00184 Rome, Italy
[2] Department of Information Engineering (DII), University of Brescia, Via Branze 38, 25123 Brescia, Italy
[3] Novosibirsk State University, Pirogova 1, Novosibirsk 630090, Russia
**mario.zitelli@uniroma1.it*

Abstract

Pioneering works on multimode fiber transmission [1,2], dated 40 years ago, predicted the existence of multimode solitons, providing conditions for the temporal trapping of the input optical modes to form a spatiotemporal soliton [3-5]. Only recently [6-8], multimode solitons were experimentally investigated in graded-index multimode fibers (GRIN), unveiling the complexity of a new, uncharted field. In our work, we experimentally and numerically investigated the propagation of ultrashort pulses over long distances of GRIN fiber. We discovered a new class of spatiotemporal solitons with surprising properties: basically single-mode, they cannot be described by the variational theory; their pulsewidth and energy are independent of the input pulse duration, and appear to depend only on the fiber dispersive parameters and, therefore, the wavelength.

The new solitons are promising for the delivery of high-energy laser beams, for high-power spatiotemporal mode-locked multimode fiber lasers, and for high-bit rate multimode fiber networks.

Main

A mysterious object came to our attention, when testing the transmission of ultrashort pulses (input pulsewidth and wavelength were 60 fs to 240 fs, and 1300 nm to 1700 nm respectively) over long spans of graded-index (GRIN) optical fiber (see Methods – Experiments). When coupling exactly on the fiber axis, with 15 μm input beam waist, we could excite 3 axial-symmetric modes, that will be addressed from now on as LP_{01}, LP_{02}, LP_{03}, for familiarity with multimodal step-index fibers. The fraction of power carried by these modes was calculated by a specific software [9] to be 52%, 30%, and 18%, respectively. The input laser pulse energy ranged between 0.1 and 20 nJ.

What we observed did not seem to obey predictions of the variational theory for spatiotemporal solitons [10-12]: Fig. 1 resumes the experimental evidence after 120 m of GRIN fiber.

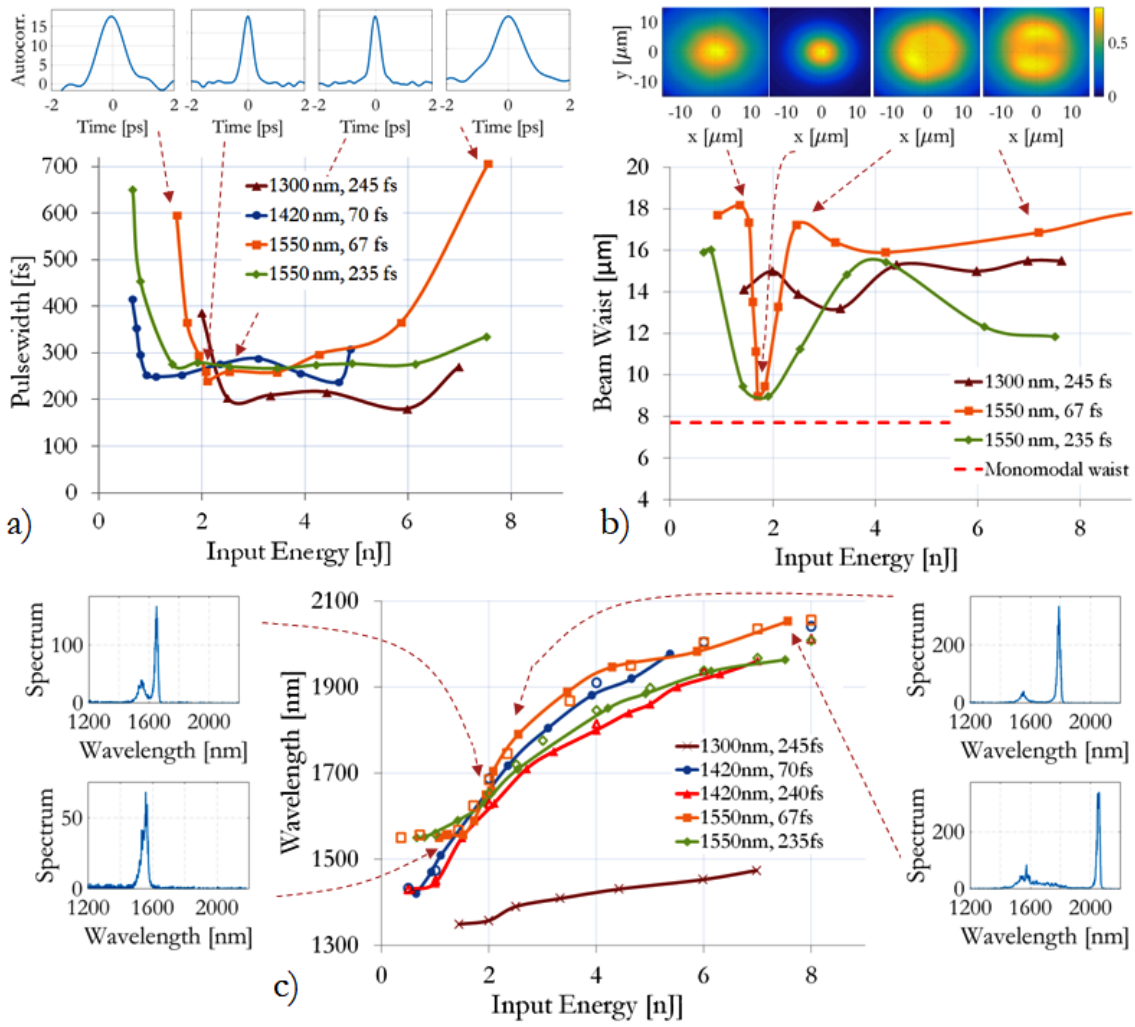

Fig. 1 – Measured soliton pulsewidth (a), beam waist (b), and wavelength (c) vs. input pulse energy, after 120 m of GRIN fiber, for different input wavelengths and pulse durations. The insets are the measured autocorrelation traces (a), output near-fields (b), and spectra (c), for input wavelength 1550 nm and pulsewidth 67 fs.

By testing different input wavelengths (1420 to 1550 nm) and input pulse widths (67 to 245 fs), spatiotemporal solitons with a common minimum pulsewidth of 260 fs were observed at the fiber output, for values of the input pulse energy ranging from 2 nJ up to 4 nJ (Fig. 1a). The case of a 1300 nm input wavelength represented an exception, which resulted into a minimum pulsewidth of 200 fs at higher energy.

The output beam waist (Fig. 1b) was severely reduced from its input value (down to a value of 8.5 μm, which is close to the theoretical value of 7.7 μm for the fundamental fiber mode), in correspondence of the input energy leading to minimum output pulsewidth. In this regime, the output beam shape was substantially monomodal, with a measured M^2=1.45, against the value of 1.3 of the input beam. The curve of the beam waist vs. energy was much narrower for input short (67 fs) pulses than for long (235 fs) pulses. Also for the beam waist, the case of 1300 nm represented an exception, with no significant beam reduction.

The output soliton wavelength (Fig. 1c) was severely affected by Raman soliton self-frequency shift (SSFS) [13, 7]. Still, the case of 1300 nm represented an exception, that provided reduced values of SSFS.

In all cases, numerical simulations performed with a coupled-mode equations model (see Methods – Simulations) fully confirmed the experimental results (empty dots).

Experimental evidence with shorter and longer spans of GRIN fiber (Fig. Supplementary 1) provided less stringent requirements for the optimal soliton energy when the fiber length is reduced. In particular, for short spans (e.g., 2 m or 10 m) the output pulsewidth remained constant for input pulse energies greater than 2.5 nJ.

What was this strange object? The minimum output pulsewidth, at 120 m distance, appeared to be independent on the input pulsewidth and wavelength, and occurred at comparable input energies in all cases. Why was the case at 1300 nm different? We decided to investigate this, starting from simulations.

Fig. 2 is a numerical representation of the evolution of an input 235 fs pulse, composed of 3 axial modes, propagating over 120 m of GRIN fiber, at the optimal input energy of 2.5 nJ. During their propagation, the 3 non-degenerate modes remain temporally trapped; the mode LP_{01} acts as an attractor for other modes, owing to non-phase

matched, asymmetrical inter-modal four-wave mixing (IM-FWM), and to inter-modal stimulated Raman scattering (SRS) [14]; at the output, a monomodal bullet remains. The pulse carried by the fundamental or LP_{01} mode experiences SSFS, while it traps and captures a large portion of energy carried by higher-order modes (HOMs).

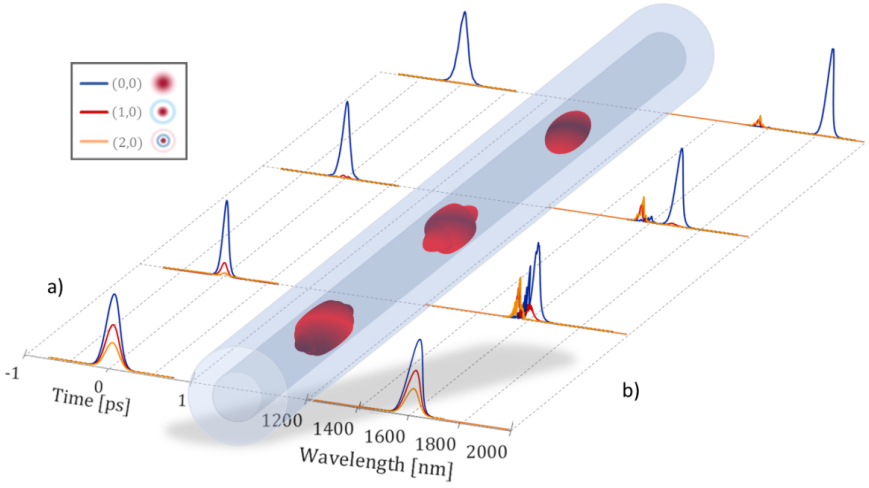

Fig. 2 – Spatiotemporal soliton formed from an input 235 fs pulse, composed by 3 axial modes, propagating over 120 m of GRIN fiber, at an optimal input energy of 2.5 nJ. a): modes power, b): modes spectra.

Fig. 3 is a numerical simulation that sheds light on the mysterious process of soliton formation. Pulses launched with either 67 fs or 235 fs input pulse widths are compared, for different input wavelengths (1350, 1550 or 1680 nm). In each case, the optimal input energy that produces a minimum pulsewidth at 120 m was chosen; in all cases, it ranges between 2 nJ and 3 nJ when going from shorter to longer wavelengths. This energy remains the same for both initial pulse widths of 67 fs or 235 fs, respectively. In all cases, two pulses with the same wavelength and different initial pulsewidth form a soliton with identical initial pulsewidth T_{s0}. The necessary propagation distance for soliton formation is 1 m at 1350 nm (and, not shown, at 1300 nm and 1420 nm), and 6

m for both 1550 nm and 1680 nm. As the soliton propagates, its pulsewidth increases because of SSFS, which increases its wavelength, and local fiber dispersion, so that the soliton condition is maintained [3,15,16]. For longer distances, the pulsewidth differences, which are observed in Fig. 3 for the several input wavelengths, approach to a common value, as experimentally confirmed at 120 m (see Fig. 1b).

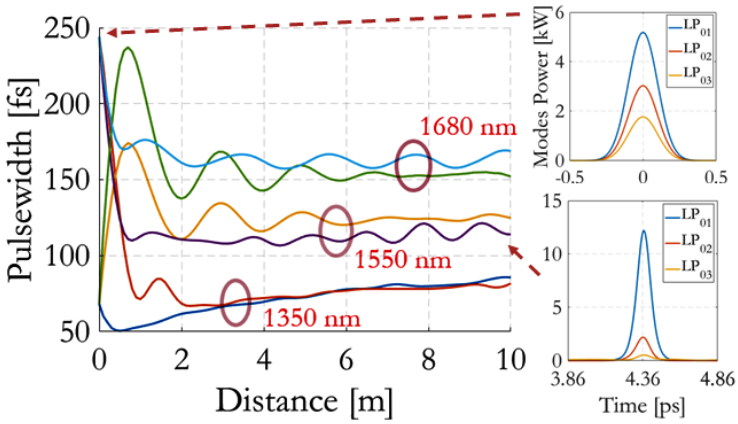

Fig. 3 – Simulated soliton pulse widths for input pulses of 67 fs and 235 fs duration, and input wavelengths of 1350 nm, 1550 nm, 1680 nm, respectively. The input modes are LP_{01}, LP_{02}, LP_{03}. Right insets: modal powers at the fiber input (top), and after 10 m of propagation (bottom), for 1550 nm input wavelength and 235 fs input pulsewidth.

The mystery was beginning to reveal itself. Input pulses with the same wavelength, comparable energies, and different pulse widths, all generate after a few meters of propagation a spatiotemporal soliton with common pulsewidth T_{s0}. T_{s0} increased for growing values of the input wavelength. Once that the spatiotemporal soliton was formed, a slow energy transfer into the LP_{01} mode was experimentally observed, while it simultaneously experiences SSFS (Fig. 1c). For distances larger than 100 m, the generated soliton appeared to be intrinsically monomodal, with a near-field waist approaching that of the fundamental mode of the MMF (Fig. 1b). For all tested

wavelengths and pulse widths, a long-distance soliton was always observed for comparable input energies (i.e., between 2 nJ and 3 nJ in the case of initial excitation of 3 axial modes). Numerical simulations (Supplementary Fig. 2) and experiments (not shown) confirmed that similar monomodal solitons are observed when launching a larger number of degenerate and non-degenerate modes at the fiber input, by varying the input beam size or angle.

Taking courage, we tried to find an analytical explanation to the mystery of the T_{s0} soliton. From numerical simulations, we know the wavelength dependence of the fiber dispersion parameters of different fiber modes. Specifically, we know the group velocities, say, $\beta_{11}(\lambda), \beta_{12}(\lambda), \beta_{13}(\lambda)$ (ps/km) for the three axial modes $LP_{01}, LP_{02}, LP_{03}$, as well as their group velocity dispersion (GVD) $\beta_2(\lambda)$ (ps^2/km), which can be assumed to be equal for all of the 3 modes. The resulting weighted mean of the group velocity difference can be written as: $\overline{\Delta\beta_1} = \left[0.30\left(\beta_{12}(\lambda) - \beta_{11}(\lambda)\right) + 0.18\left(\beta_{13}(\lambda) - \beta_{11}(\lambda)\right)\right]/(0.30 + 0.18)$.

We recall now the following characteristic lengths:

i) The mean modal walk-off length of the forming soliton $L_W = T_0/\overline{\Delta\beta_1}$, with $T_0 = T_{s0}/1.763$, defined as the distance where, in the linear regime, the modes separate temporally.

ii) The pulse nonlinearity length L_{NL} and its dispersion length $L_D = T_0^2/|\beta_2(\lambda)|$, defined as the characteristic length scales for Kerr nonlinearity and chromatic dispersion, respectively.

iii) The random mode coupling and birefringence correlation lengths, L_{cm} and L_{cp}, which are the characteristic length scales associated with linear coupling between degenerate modes or between polarizations, respectively [17-19].

In order to explain the mystery, we may assume that, when nonlinearity acts over distances shorter than those associated with random mode coupling and birefringence, i.e., for $L_{NL} < L_{cm}, L_{cp}$, it is possible to observe a spatiotemporal soliton which is attracted into an effectively single-mode soliton [14]. A second requirement to be considered is that both of the dispersion and nonlinearity lengths are comparable with the fiber walk-off length: $L_D = L_{NL} = const \cdot L_W$, being *const* an adjustment constant. A similar condition for temporal trapping of the optical modes was initially predicted, for the j-th mode, by [1,2] as $L_{Wj} \leq L_D = L_{NL}$.

Based on the above considerations, we may find the condition to be respected by the soliton pulsewidth at the distance of initial formation

$$T_{S0}(\lambda) = const \cdot 1.763 \frac{|\beta_2(\lambda)|}{\Delta\beta_1(\lambda)} \quad . \tag{1}$$

We measured the forming soliton pulsewidth at 1 m of distance (at 1300, 1350, and 1420 nm) and at 6 m of distance (at 1550, 1680nm), for the optimal input energies of 2 to 3 nJ, and input pulse widths ranging between 61 and 96 fs (depending on the input wavelength). We compared experimental results with numerical simulations at different input wavelengths and input pulsewidth of 67 fs and 235 fs, and with the theoretical curve of T_{s0} upon wavelength as it is obtained from Eq. 1, by using the dispersion curves of a GRIN fiber. The corresponding results are shown in Fig. 4, confirming the good agreement between theory and experiments/simulations, provided the adjustment constant is set to $const = 0.87$, and for wavelengths above 1350 nm (the $const$ value may change with the coupling conditions). Whereas for wavelengths below 1350 nm, the (anomalous) dispersion becomes very small, and the theory fails in

predicting solitons with unphysical short pulse durations, also because we neglect the presence of higher-order dispersion terms.

Therefore, Eq. 1 confirms that a spatiotemporal soliton may be formed from the initial pulse, eventually leaving behind a certain amount of energy in dispersive waves. The soliton initial pulsewidth, and therefore energy, depends on the fiber dispersion parameters. Our mysterious solitonic object appears to be clamped to the fiber walk-off length L_W. The soliton pulsewidth T_{s0}, at its formation distance, varies with the wavelength of the input pump pulse, but its value turns out to be independent of input pulse duration. From Fig. 4, we find that a soliton with duration longer than few hundreds of femtoseconds cannot arise from non-degenerate modes.

For relatively long input pulses (e.g., a 10 ps input pulse carried by 15 modes, as in the example of Supplementary Fig. 3), groups of modes separate temporally. However, in this case, it is still possible to inject the proper energy in each group of degenerate modes, in order to obtain the generation of several independent spatiotemporal solitons.

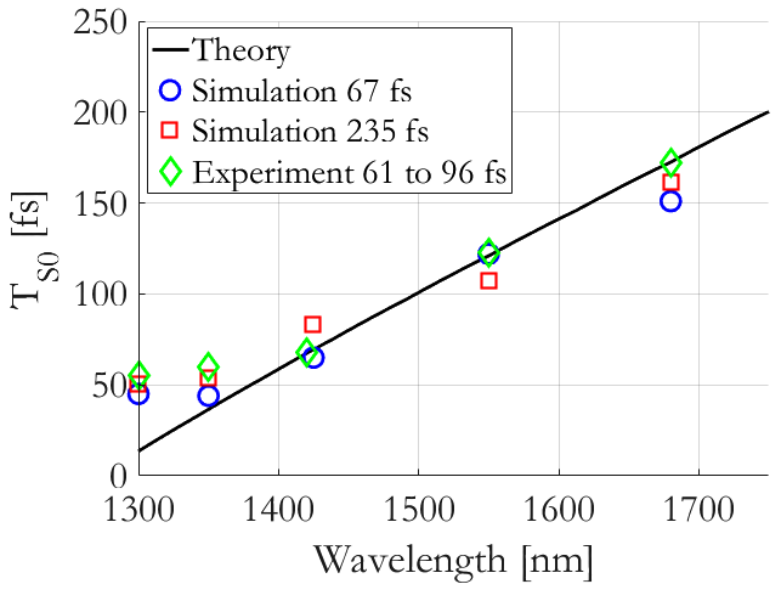

Fig. 4 – Theoretical curve of soliton pulse duration vs. wavelength, compared with measured and simulated soliton pulse widths. Experiments carried out with 1 m of GRIN fiber, with input wavelengths and pulse widths: 1300 nm and 61 fs, 1350 nm and 61 fs, 1420 nm and 70 fs. Experiment carried out with 6 m of GRIN fiber, with input wavelength and pulse widths: 1550 nm and 67 fs, 1680 nm and 96 fs. Simulations were carried out with same distances and input wavelengths, and pulse widths of 67 fs and 235 fs.

The unique properties of walk-off solitons can be advantageously used to develop high-power spatiotemporal mode-locked multimode fiber lasers, with pulses of fixed duration at a given wavelength. The additional ability to form a single-mode beam can be used for beam delivery applications.

Methods

Simulations

Numerical simulations are based on a coupled-mode equations approach [20,21], which requires the preliminary knowledge of the input power distribution among fiber modes. The model couples the propagating mode fields via Kerr nonlinearities, by four-wave mixing (FWM) terms of the type $Q_{plmn}A_l A_m A_n^*$, being Q_{plmn} the coupling coefficients, proportional to the overlap integrals of the transverse modal field distributions, and by stimulated Raman scattering (SRS) with same coupling coefficients. Fiber dispersion and nonlinearity parameters are estimated to be $\beta_2 = -28.8$ ps^2/km at 1550 nm, $\beta_3 = 0.142$ ps^3/km; nonlinear index $n_2 = 2.7 \times 10^{-27}$ m^2/W, Raman response $h_R(t)$ with typical times of 12.2 and 32 fs [22,23]. Wavelength-dependent linear losses of silica were included.

Experiments

The experimental setup included an ultra-short pulse laser system, composed by a hybrid optical parametric amplifier (OPA, Lightconversion ORPHEUS-F), pumped by a femtosecond Yb-based laser (Lightconversion PHAROS-SP-HP), generating pulses at 100 kHz repetition rate with Gaussian beam shape ($M^2 = 1.3$); the central wavelength was tunable between 1300 nm and 1700 nm, and the pulsewidth ranged between 60 fs and 240 fs, depending on the wavelength and the insertion of pass-band filters. The laser beam was focused by a 50 mm lens into the fiber, with a $1/e^2$ input diameter of approximately 30 μm (15 μm beam waist). The laser pulse input energy was controlled by means of an external attenuator, and varied between 0.1 nJ and 20 nJ.

Care was taken during the input alignment in order to observe, in the linear regime, an output near-field that was composed by axial modes only; this could be particularly

appreciated for long lengths of GRIN fiber (120 m and more). The used fiber was a span (from 1 m to 850 m) of parabolic GRIN fiber, with core radius $r_c = 25$ μm, cladding radius 62.5 μm, cladding index $n_{clad} = 1.444$ at 1550 nm, and relative index difference $\Delta = 0.0103$.

At the fiber output, a micro-lens focused the near field on an InGaAs camera (Hamamatsu C12741-03); a second lens focused the beam into an optical spectrum analyzer (Yokogawa AQ6370D) with wavelength range 600-1700 nm, and to a real-time multiple octave spectrum analyzer (Fastlite Mozza) with a spectral detection range of 1100-5000 nm. The output pulse temporal shape was inspected by using an infrared fast photodiode, and an oscilloscope (Teledyne Lecroy WavePro 804HD) with 30 ps overall time response, and an intensity autocorrelator (APE pulseCheck 50) with femtosecond resolution.

References

1. Hasegawa, A., Self-confinement of multimode optical pulse in a glass fiber, Opt. Lett. **5**, 416–417 (1980).
2. Crosignani, B., & Di Porto, P., Soliton propagation in multimode optical fibers, Opt. Lett. **6**, 329–330 (1981).
3. Renninger, W. H., & Wise, F. W., Optical solitons in graded-index multimode fibres, Nat. Commun. **4**, 1719 (2013).
4. Ahsan, A. S. , & Agrawal, G. P., Graded-index solitons in multimode fibers, Opt. Lett. **43**, 3345–3348 (2018).
5. Krupa, K., Tonello, A., Barthélémy, A., Mansuryan, T., Couderc, V., Millot, G., Grelu, P., Modotto, D., Babin, S. A., & Wabnitz, S., Multimode nonlinear fiber optics, a spatiotemporal avenue, APL Photonics **4**, 110901 (2019).

6. Wright, L. G., Renninger, W. H., Christodoulides, D. N., & Wise, F. W., Spatiotemporal dynamics of multimode optical solitons, Opt. Express **23**, 3492–3506 (2015).

7. Zhu, Z., Wright, L. G., Christodoulides, D. N., & Wise, F. W., Observation of multimode solitons in few-mode fiber, Opt. Lett. **41**, 4819–4822 (2016).

8. Wright, L. G., Christodoulides, D. N., & Wise, F. W., Controllable spatiotemporal nonlinear effects in multimode fibers, Nat. Phot. 9, 306-310 (2015).

9. Sidelnikov, O. S., Podivilov, E. V., Fedoruk M. P., & Wabnitz S., Random mode coupling assists Kerr beam self-cleaning in a graded-index multimode optical fiber, Opt. Fiber Technol. **53**, 101994 (2019).

10. Yu, S.-S., Chien, C.-H., Lai, Y., & Wang, J., Spatio-temporal solitary pulses in graded-index materials with Kerr nonlinearity, Opt. Commun. **119**, 167–170 (1995).

11. Raghavan, S., & Agrawal, G. P., Spatiotemporal solitons in inhomogeneous nonlinear media, Opt. Commun. **180**, 377 – 382 (2000).

12. Karlsson, M., Anderson, D., and Desaix, M., Dynamics of self-focusing and self-phase modulation in a parabolic index optical fiber, Opt. Lett. **17**, 22–24 (1992).

13. Grudinin, A. B., Dianov, E., Korbkin, D., Prokhorov, A. M., & Khaidarov, D., Nonlinear mode coupling in multimode optical fibers; excitation of femtosecond-range stimulated-Raman-scattering solitons, J. Exp. Theor. Phys. Lett. 47, 356–359 (1988).

14. Zitelli, M., Ferraro, M., Mangini, F., & Wabnitz, S., Singlemode spatiotemporal soliton attractor in multimode GRIN fibers, Photonics Research, in press (2021).

15. Hasegawa, A., & Matsumoto, M., *Optical Solitons in Fibers* (Springer, 2003).

16. Zakharov, V. E., & Wabnitz, S., *Optical Solitons: Theoretical Challenges and Industrial Perspectives* (Springer, 1999).

17. Ho, K., & Kahn, J., Linear propagation effects in mode-division multiplexing systems, J. Light. Technol. **32**, 614–628 (2014).

18. Mumtaz, S., Essiambre, R.-J., & Agrawal, G. P., Nonlinear propagation in multimode and multicore fibers: generalization of the Manakov equations, J. Lightwave Technol. 31, 398–406 (2012).
19. Xiao, Y., Essiambre, R.-J., Desgroseilliers, M., Tulino, A. M., Ryf, R., Mumtaz, S., & Agrawal, G. P., Theory of intermodal four-wave mixing with random linear mode coupling in few-mode fibers, Opt. Express 22, 32039–32059 (2014).
20. Poletti, F., & Horak, P., Description of ultrashort pulse propagation in multimode optical fibers, J. Opt. Soc. Am. B 25, 1645–1654 (2008).
21. Wright, L. G., Ziegler, Z. M., Lushnikov, P. M., Zhu, Z., Eftekhar, M. A., Christodoulides, D. N., and Wise, F. W., Multimode nonlinear fiber optics: massively parallel numerical solver, tutorial, and outlook, IEEE J. Sel. Top. Quantum Electron. 24, 1–16 (2018).
22. Stolen, R. H., Gordon, J. P., Tomlinson, W. J., & Haus, H. A., Raman response function of silica-core fibers, J. Opt. Soc. Am. B 6, 1159–1166 (1989).
23. Agrawal, G. P., *Nonlinear Fiber Optics*, 3rd ed., Par. 2.3 (Academic, 2001).

Acknowledgements

We wish to thank Dr. Cristiana Angelista for her valuable help in narrative restyling of this letter.

We acknowledge the financial support from the European Research Council Advanced Grants No. 874596 and No. 740355 (STEMS), the Italian Ministry of University and Research (R18SPB8227), and the Russian Ministry of Science and Education Grant No. 14.Y26.31.0017.